Nanoscale Research Letters
a SpringerOpen Journal

NANO EXPRESS   **Open Access**

Oxygen-containing functional group-facilitated CO_2 capture by carbide-derived carbons

Wei Xing[1*], Chao Liu[1], Ziyan Zhou[2], Jin Zhou[2], Guiqiang Wang[2], Shuping Zhuo[2], Qingzhong Xue[1], Linhua Song[1] and Zifeng Yan[1*]

Abstract

A series of carbide-derived carbons (CDCs) with different surface oxygen contents were prepared from TiC powder by chlorination and followed by HNO_3 oxidation. The CDCs were characterized systematically by a variety of means such as Fourier transform infrared spectroscopy, X-ray photoelectron spectroscopy, ultimate analysis, energy dispersive spectroscopy, N_2 adsorption, and transmission electron microscopy. CO_2 adsorption measurements showed that the oxidation process led to an increase in CO_2 adsorption capacity of the porous carbons. Structural characterizations indicated that the adsorbability of the CDCs is not directly associated with its microporosity and specific surface area. As evidenced by elemental analysis, X-ray photoelectron spectroscopy, and energy dispersive spectroscopy, the adsorbability of the CDCs has a linear correlation with their surface oxygen content. The adsorption mechanism was studied using quantum chemical calculation. It is found that the introduction of O atoms into the carbon surface facilitates the hydrogen bonding interactions between the carbon surface and CO_2 molecules. This new finding demonstrated that not only the basic N-containing groups but also the acidic O-containing groups can enhance the CO_2 adsorbability of porous carbon, thus providing a new approach to design porous materials with superior CO_2 adsorption capacity.

Keywords: Carbide-derived carbons; CO_2 adsorption; Oxidation

Background

Observational evidence proved that global warming has already caused a series of severe environmental problems such as sea level rise, glacier melt, heat waves, wildfires, etc. [1,2]. These disasters have already greatly damaged the balance of nature. It is widely believed that the global warming in recent years is mainly ascribed to the excessive emission of greenhouse gases, in which CO_2 is the most important constituent. According to the Fourth Assessment Report which was published by Intergovernmental Panel on Climate Change (IPCC) in 2007, the annual emissions of CO_2 have grown from 21 to 38 gigatonnes (Gt) and the rate of growth of CO_2 emissions was much higher during 1995 to 2004 (0.92 Gt per year) than that of 1970 to 1994 (0.43 Gt per year) [3]. So, it is urgent to develop CO_2 capture and storage (CCS) technologies [4].

In an early stage, people used to trap CO_2 in some geological structures such as depleted oil and gas reservoirs, deep saline aquifers, unminable coal beds, etc. [5-7]. However, CO_2 geological storage usually requires large-scale equipment which calls for great costs. On the other hand, there is an obstacle to reuse the CO_2, which has been trapped in these geological structures, as an industrial raw material due to its low purity grade. So, it is necessary to develop a more feasible CCS technology.

The application of porous materials in the capture and storage of CO_2 has a big potential and wide prospect. There are many kinds of porous materials that can be used as CO_2 adsorbents, such as molecular sieves, porous silica, metal organic frameworks (MOFs), and porous carbons [8-18] due to their attractive properties such as high specific surface area and highly developed pore structure. Among these porous materials, porous carbons are especially attractive because they are inexpensive, easy to regenerate, and not sensitive to moisture which may compete with CO_2 when adsorption happens [19-21]. However, it is hard for pristine porous carbon materials

* Correspondence: xingwei@upc.edu.cn; zfyancat@upc.edu.cn
[1]State Key Laboratory of Heavy Oil Processing, School of Science, China University of Petroleum, Qingdao 266580, People's Republic of China
Full list of author information is available at the end of the article

Springer

without any modification to reach high CO_2 uptake values [22]. As a result, researchers modified the surface of porous carbon with nitrogen-containing functional groups [23], which enhanced the CO_2 adsorption capacity of these porous carbon materials. For example, Chandra et al. synthesized a kind of N-doped carbon by chemical activation of polypyrrole functionalized graphene sheets. This kind of carbon material showed a CO_2 uptake of 4.3 mmol g^{-1} with high selectivity at 298 K under 1 atm [24]. Zhou et al. prepared a series of N-doped microporous carbons using zeolite NaY as a hard template and furfuryl alcohol/acetonitrile as carbon precursors. The CO_2 adsorption capacity of as-prepared N-doped carbons was much higher than that of the template carbons without N-doping [25]. Nandi et al. prepared a series of highly porous N-doped activated carbon monoliths by physical activation. The monoliths exhibit an excellent CO_2 uptake of up to 5.14 mmol g^{-1} at ambient temperature and 11.51 mmol g^{-1} at 273 K under atmospheric pressure [26]. Wu et al. synthesized a series of nitrogen-enriched ordered mesoporous carbons via soft-template method. The CO_2 adsorption capacity of nitrogen-enriched carbon is higher than that of pristine material due to the presence of nitrogen-containing functionalities [27]. Sevilla et al. prepared a series of N-doped porous carbons using KOH as activation agent and polypyrrole as carbon precursor. The excellent CO_2 uptakes of these carbons were ascribed to the abundant micropores with the pore size around 1 nm and the presence of basic N-containing groups [19]. Hao et al. synthesized a kind of nitrogen-containing carbon monolith through a self-assembled polymerization of resol and benzoxazine followed by carbonization. The high CO_2 adsorption capacity was attributed to the N-containing groups of the resulting carbons [21]. The above-mentioned works all proved that the presence of nitrogen-containing functional groups can enhance the CO_2 adsorption capacities of porous carbons, and all these authors simply attribute this adsorption-enhancing effect to the acid-base interactions between acidic CO_2 molecules and basic N-containing groups without providing any experimental evidence. However, for these N-doped porous carbons that are prepared at high temperatures, the N atoms reside in the carbon skeleton and are stable at high temperatures. The basicity of these N-containing functional groups is very much weaker than that of organic amines and is rarely studied in the literatures. To the best of our knowledge, there is no direct experimental evidence to prove that this acid-base interaction does exist between CO_2 molecules and the N-containing groups of the N-doped carbon. Our previous research has proved that this CO_2 adsorption-enhancing effect for N-doped carbon is due to the hydrogen bonding interactions between CO_2 molecules and H atoms on the carbon surface. This hydrogen

bonding interactions are facilitated efficiently by N-doping, which challenges the acid-base interacting mechanism generally accepted in this field [28].

In this paper, the influence of oxygen-containing groups of the porous carbon on CO_2 capture property is studied for the first time. It is found that the presence of oxygen-containing functional groups can enhance the CO_2 adsorption capacity of porous carbons. As evidenced by both quantum chemical calculations and a variety of characterization means, this adsorption-enhancing effect is attributed to the hydrogen bond interactions between hydrogen atoms on the carbon surface and CO_2 molecules, which is greatly enhanced by the presence of O atoms on the carbon surface. As we know, most oxygen-containing functional groups such as phenolic hydroxyl groups, carboxyl groups, lactone groups, and aldehyde groups show acid tendency [29]. According to the acid-base interacting mechanism currently accepted in this field, the presence of such acidic groups would show a negative effect on CO_2 adsorption. Therefore, our work challenges the acid-base interacting mechanism currently accepted in this field. Our new finding also provides a new approach to design porous materials with superior CO_2 adsorption capacity.

Methods
Material preparation
The carbide-derived carbons (CDCs) were prepared by chlorinating TiC according to the literatures [30,31]. In the preparation, the TiC powder was placed in a quartz boat and then loaded into a quartz tube furnace. First, the quartz tube with a quartz boat inside was purged with nitrogen to thoroughly dispel oxygen. Then, the temperature of the furnace was raised to 700°C by 5°C min^{-1} under nitrogen flow (40 mL min^{-1}). Afterwards, the nitrogen flow was shifted to chlorine flow (15 mL min^{-1}) for 3 h. The resulting powder was annealed under hydrogen at 600°C for 2 h to remove residual chlorine and chlorine-containing compounds.

To investigate the influence of oxygen content on CO_2 adsorption capacity, the as-prepared CDC was placed in a flask followed by the addition of 25 mL concentrated nitric acid for oxidation. After stirring under different temperatures for 3.5 h, the obtained carbon powder was washed thoroughly with deionized water. The dried sample was named as CDC-x, where x represents the oxidation temperature. The reduced carbon samples were obtained by heating CDC-x in H_2 atmosphere at 800°C for 3 h and were denoted as CDC-x-HR.

Material characterization
The pore structure parameters and CO_2 adsorption capacities of the carbon samples were analyzed with a surface area and porosity analyzer (ASAP 2020, Micromeritics

Corp., Norcross, GA, USA). Nitrogen sorption isotherms and CO_2 adsorption isotherms were determined at 77 and 298 K, respectively. The carbon samples were strictly degassed under vacuum (0.2 Pa) at 350°C overnight before sorption measurements. N_2 and CO_2 gases with super high purity (99.999%) were used for the sorption measurements. The specific surface area and micropore volumes of the carbons were measured by Brunauer-Emmett-Teller (BET) method and t-plot method, respectively. The single-point total pore volume was measured at $p/p_0 = 0.995$ and the average pore size was equal to $4V_{total}/S_{BET}$. Microscopic morphologies of the carbons were observed using a transmission electron microscope (TEM, Hitachi H800, Chiyoda, Tokyo, Japan). The chemical compositions of the carbons were determined using both a Vario EI IIIb element analyzer and an energy dispersive spectrometer (EDS; INCA Energy, Oxford, Buckinghamshire, UK). The surface chemical property of the carbons was analyzed by a X-ray photoelectron spectroscope (XPS; PHI-5000 Versaprobe, Chanhassen, MN, USA) using a monochromated Al Kα excitation source. The binding energies were calibrated with respect to C1s (284.6 eV). Fourier transform infrared spectroscopy (FT-IR) analyses were carried out on a Nicolet 5800 infrared spectrometer (Madison, WI, USA) with an accuracy of 0.09 cm^{-1}. The carbons were first mixed with KBr at a mass ratio of 1/100 and then ground in an agate mortar for pressing KBr pellets.

Results and discussion

Surface properties and pore structure of carbon samples

FT-IR was used to identify oxygen-containing functional groups of the CDC samples. Compared with the pristine CDC sample before oxidation, the FT-IR spectrum of CDC-50 (Additional file 1: Figure S1) shows some new characteristic bands that were introduced by HNO_3 oxidation. The band at 3,200 to 3,600 cm^{-1} was attributed to hydroxyl groups. The band at around 1,710 cm^{-1} was attributed to -C = O stretching vibration. The peaks between 1,000 to 1,300 cm^{-1} can be assigned to -C-O stretching and -OH bending modes of alcoholic, phenolic, and carboxylic groups. All this new emerging bands indicate that HNO_3 oxidation introduced a large number of oxygen-

containing functional groups, such as hydroxyl, carbonyl, and carboxyl groups, to the CDC [32-34].

Moreover, elemental analysis (EA), EDS, and XPS were employed to intensively investigate the oxygen content of the carbons. As is shown in Table 1, all these three characterization means undoubtedly demonstrate that HNO_3 oxidation did introduce a large quantity of oxygen atoms to the carbon; HNO_3 oxidation at higher temperature would introduce more oxygen atoms to the carbon; the subsequent H_2 reduction can effectively remove oxygen atoms from the oxidized carbons. For instance, as for EA data, the oxygen content of the carbons increased from 17.6 to 36.7 wt% and 41.5 wt% after oxidizing pristine CDC by HNO_3 at 50°C and 80°C, respectively. The subsequent H_2 reduction decreased the oxygen contents to 11.2 and 20.5 wt% for CDC-50 and CDC-80, respectively.

Nitrogen physisorption measurements were performed at 77 K to characterize the surface areas and pore structures of CDCs. The N_2 adsorption isotherms of all the carbons (Additional file 1: Figure S2) exhibit type I isotherms, and no hysteresis loop can be observed for these samples, indicating the microporous nature of these carbons and the absence of mesopores. The detailed specific surface area and pore structure parameters of these carbons are listed in Table 1. The specific surface area and micropore volume decrease from 1,216 m^2/g and 0.59 cm^3/g to 907 m^2/g and 0.43 cm^3/g, respectively, after oxidizing the pristine CDC by HNO_3 at 50°C, which is due to the introduction of oxygen-containing groups to the pore surface of the carbon. After H_2 reduction, the specific surface area and micropore volume increase back to 1,115 m^2/g and 0.51 cm^3/g, indicating that the oxygen-containing groups are effectively removed from the pore surface by H_2 reduction. This result coincides with the elemental analyses data. It is also suggested that the oxidation of the pristine CDC by HNO_3 at 50°C did not obviously damage the pore structure of the carbon and that the decrement in the specific surface area and micropore volume due to the oxidation can be mostly recovered by H_2 reduction. By contrast, oxidizing the pristine CDC by HNO_3 at 80°C results in the dramatic

Table 1 Specific surface areas, pore structure parameters, and oxygen contents of CDCs

Sample	S_{BET}[a]	V_{micro}[b]	V_{total}[c]	Pore size[d]	O content		
	$(m^2 g^{-1})$	$(cm^3 g^{-1})$	$(cm^3 g^{-1})$	(nm)	EA (wt%)	XPS (wt%)	EDS (wt%)
Pristine CDC	1,216	0.59	0.65	2.13	17.6	8.7	6.8
CDC-50	907	0.43	0.47	2.06	36.7	14.6	20.3
CDC-50-HR	1,115	0.51	0.58	2.08	11.2	10.2	10.3
CDC-80	449	0.22	0.24	2.15	41.5	15.7	29.8
CDC-80-HR	497	0.22	0.27	2.21	20.5	14.2	16.0

[a]BET specific surface area. [b]Micropore volumes calculated by the t-plot method. [c]Single-point total pore volume measured at $p/p_0 = 0.995$. [d]Pore size = $4V_{total}/S_{BET}$.

decrease of the specific surface area and micropore volume. Although the subsequent H_2 reduction can effectively remove oxygen-containing groups from CDC-80, the surface area and micropore volume cannot be recovered, indicating that HNO_3 oxidation at 80°C severely damaged the micropore structure of the carbon.

In order to further clarify the pore structure evolution caused by HNO_3 oxidation, TEM observations were also conducted to get the microscopic morphology of the CDC. The pristine CDC (Figure 1a) shows amorphous structure and abundant micropores that are formed by the stacking of curved graphene layers. The samples CDC-50 and CDC-80 (Figure 1b,c) show similar microscopic morphology to the pristine CDC, suggesting the microporous nature of all the three samples. These results coincide with the pore size data shown in Table 1.

CO_2 capture performances of the CDCs

According to classical gas adsorption theories, gas adsorption on porous carbons usually relies on the highly developed microporous structure and large specific surface area. Recent studies also demonstrated that micropores (<1 nm) are beneficial to CO_2 adsorption for porous materials [18,35-38]. In this work, CDC-50 shows lower specific area and micropore volume (Table 1 and Figure 1d) than the pristine CDC and CDC-50-HR. However, as shown in Figure 2a, CDC-50 (3.87 mmol g^{-1} under 1 atm) possesses an apparently higher CO_2 uptake than the pristine CDC (3.66 mmol g^{-1} under 1 atm) and CDC-50-HR (2.63 mmol g^{-1} under 1 atm). Likewise, CDC-80 has a lower specific surface area and the same micropore

volume than/as its reduced product CDC-80-HR. However, the former (2.71 mmol g^{-1} under 1 atm) possesses an obviously higher CO_2 uptake than the latter (1.63 mmol g^{-1} under 1 atm). As for CDCs, their CO_2 uptakes do not have a linear correlation with their micropore volume, as is shown in Figure 2b inset. So, the CO_2 adsorption results for the CDCs cannot be explained by classical adsorption theories. Nevertheless, it is very instructive to find that the CO_2 uptakes per unit surface area of the carbons are positively related to the oxygen content of the carbons (Figure 2b), indicating that the CO_2 adsorption capacity of the carbons was greatly facilitated by the introduction of oxygen-containing groups to the carbon. This result agrees well with the work of Liu [5].

In order to reveal the effect of oxygen-containing groups on CO_2 adsorption for the carbons, a theoretical carbon surface model (OCSM) containing six different typical O-containing functional groups was developed in light of Niwa's model [39]. A pure carbon model without oxygen atoms (CSM) was also devised for comparison, as is shown in Figure 3. Density functional theory B3LYP was employed to study the interactions between these models and CO_2, and all the configurations were optimized with the 6-31 + G* basis set for all atoms using the Gaussian-03 suite package [40].

The optimized results at the 6-31 + G* level are that there are six OCSM-CO_2 complexes and six CSM-CO_2 complexes. Furthermore, the calculated results demonstrate that the frequency values of all complexes are positive, showing that they are in stable configurations. Additional file 1: Figure S3 illustrates the geometric
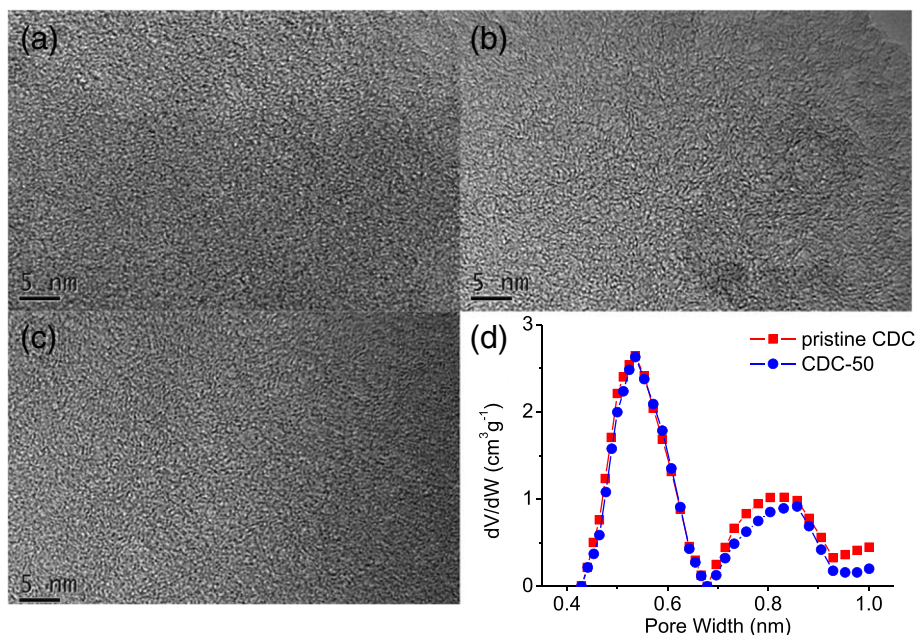

Figure 1 TEM images of CDCs: (a) CDC, (b) CDC-50, and (c) CDC-80, and (d) micropore size distribution of CDCs.
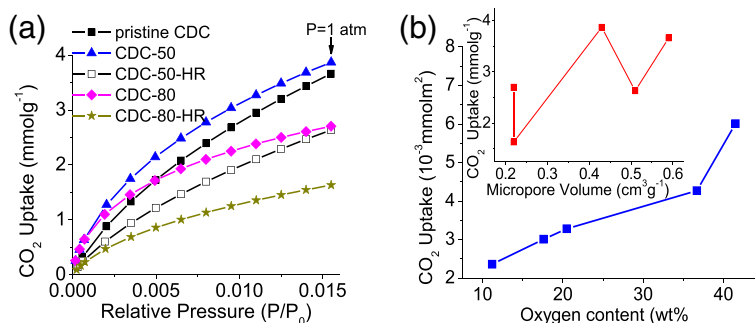
Figure 2 CO_2 adsorption isotherms for the CDCs (a) and a plot of CO_2 uptake vs. oxygen content (b). The inset is a plot of CO_2 uptake vs. micropore volume.

configurations for all the complexes, and Additional file 1: Table S1 tabulates the total energies for all the complexes. In these complexes, hydrogen bonds between CO_2 and OCSM/CSM are formed due to the high electronegativity of the oxygen atom in the CO_2 molecule. This type of weak hydrogen bond has been widely studied in recent years. The experimental and theoretical studies have demonstrated its existence although the interaction of C-H···O is weaker than that of typical hydrogen bonds such as O-H···O and N-H···O [41-43].

Computational results indicated that the binding energies for such hydrogen bonds are different at various positions. It is apparent that the larger the bonding
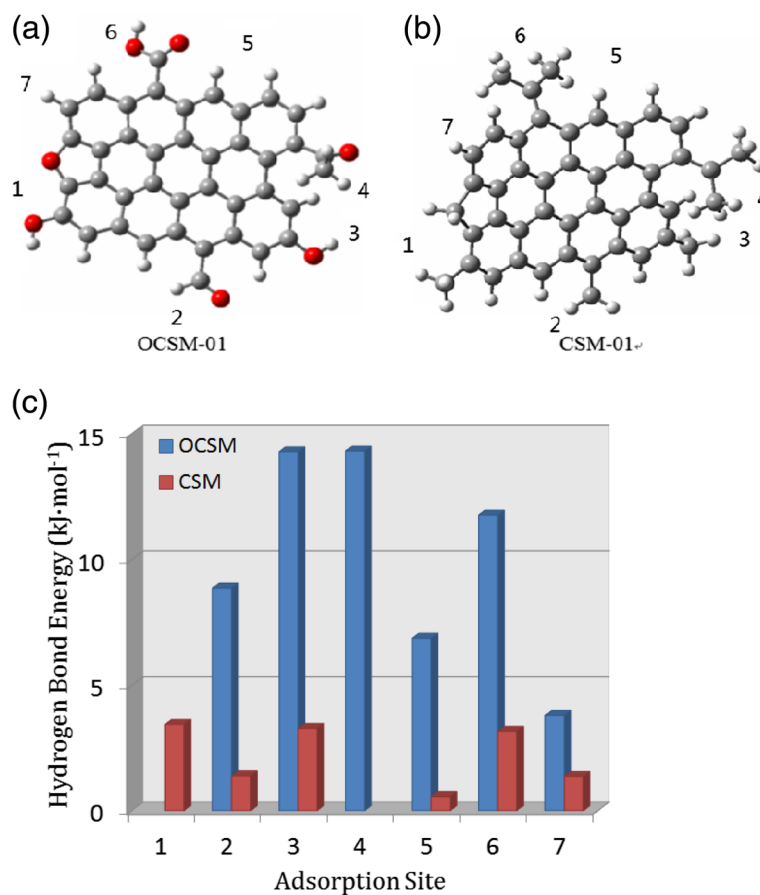
Figure 3 Theoretical carbon models and hydrogen bond energies. Theoretical models for **(a)** oxygen-containing carbon surface and **(b)** pure carbon surface (red ball: oxygen atom; grey ball: carbon atom; small grey ball: hydrogen atom). **(c)** Hydrogen bond energies at different adsorption sites.

energy ΔE (kJ mol^{-1}), the stronger the adsorption affinity. The average binding energy of six OCSM-CO$_2$ complexes is 9.98 kJ mol^{-1}, and that of CSM-CO$_2$ complexes is 2.20 kJ mol^{-1}, suggesting that the hydrogen bonds in the OCSM-CO$_2$ complexes are much stronger than those in CSM-CO$_2$ complexes. This binding energy difference (7.78 kJ mol^{-1}) between OCSM-CO$_2$ and CSM-CO$_2$ complexes roughly agrees with the difference of CO$_2$ adsorption heat between the pristine CDC and CDC-50 (as shown in Additional file 1: Figure S4), which somewhat reflects the effect of oxygen introduction on CO$_2$ adsorption heat for the CDCs.

In order to prove the existence of the hydrogen bonding interactions between the carbon and CO$_2$ molecules, FT-IR spectra (Figure 4) were recorded for CDC-50 under both N$_2$ and CO$_2$ atmospheres using a Nicolet 5700 infrared spectrometer with an accuracy of 0.1 cm^{-1}. Under N$_2$ atmosphere, the peak at 2,921.68 cm^{-1} was attributed to the C-H anti-symmetric stretching vibration. When the atmosphere was shifted to CO$_2$, this peak was broadened

and redshifted to low wavenumber, 2,919.52 cm^{-1}. The already published papers proved that hydrogen bonding interactions can weaken the C-H bonding energy, which lead to the redshift of corresponding peak on the FT-IR spectra [44,45]. This phenomenon confirms that the hydrogen bonding interactions between CDC-50 and CO$_2$ molecules do exist. Unfortunately, due to the interference caused by adsorbed water moisture on the carbon samples in FT-IR measurements, the effects of hydrogen bonding on O-H and C-O bonds cannot be observed. Besides, elemental analyses show that HNO$_3$ oxidation can increase the H content from 13 to 33 mmol g^{-1} for the pristine CDC and CDC-50, respectively, which enables more hydrogen bonding interactions between CDC-50 and CO$_2$ molecules. This also explains why the oxidized CDC samples possess higher CO$_2$ uptakes.

Conclusions

We intensively investigated the effect of introducing oxygen-containing functional groups to the carbon surface on the CO$_2$ uptake of CDCs. Structural characterizations and CO$_2$ adsorption on the CDCs indicate that CO$_2$ uptake is independent of the specific surface area and micropore volume of the CDCs but closely related to the oxygen content of the carbons. Quantum chemical calculations and FT-IR measurements reveal that the introduction of oxygen atoms into a carbon surface facilitates the hydrogen bonding interactions between the carbon surface and CO$_2$ molecules, which accounts for the enhanced CO$_2$ uptake on the oxidized CDCs. Because most oxygen-containing functional groups show acidic tendency, this new finding challenges the 'acid-base interacting mechanism' generally accepted in this field. This new finding also provides a new approach to design porous carbon with superior CO$_2$ adsorption capacity.

Additional file

Additional file 1: Supporting information. Table S1. the total energies for OCSM-CO$_2$ and CSM-CO$_2$ complexes. **Table S2.** chemical composition of the CDCs determined by elemental analysis. **Figure S1.** FT-IR spectra of pristine CDC and CDC-50. **Figure S2.** nitrogen adsorption isotherms of the CDCs. **Figure S3.** geometric configurations and total energies for OCSM, CSM, OCSM-CO$_2$ complexes and CSM-CO$_2$ complexes. **Figure S4.** isosteric heats of CO$_2$ adsorption on the carbons at different CO$_2$ uptakes.
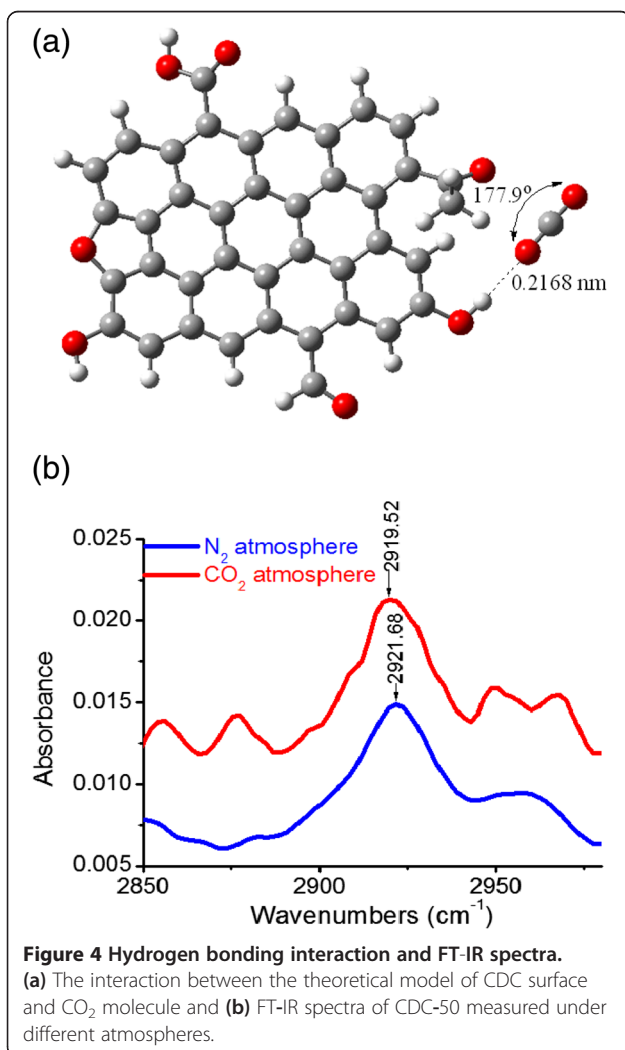

Figure 4 Hydrogen bonding interaction and FT-IR spectra. **(a)** The interaction between the theoretical model of CDC surface and CO$_2$ molecule and **(b)** FT-IR spectra of CDC-50 measured under different atmospheres.

Author details

[1]State Key Laboratory of Heavy Oil Processing, School of Science, China University of Petroleum, Qingdao 266580, People's Republic of China. [2]School of Chemical Engineering, Shandong University of Technology, Zibo 255049, People's Republic of China.

References

1. Tollefson J: **Heatwaves blamed on global warming.** *Nature* 2012, **488**:143–144.
2. Moritz MA: **Wildfires ignite debate on global warming.** *Nature* 2012, **487**:273.
3. Bernstein L, Bosch P, Canziani O, Chen Z, Christ R, Davidson O: *Climate Change 2007: Synthesis Report. An Assessment of the Intergovernmental Panel on Climate Change.* IPCC: Geneva; 2008.
4. Lund H, Mathiesen BV: **The role of carbon capture and storage in a future sustainable energy system.** *Energy* 2012, **44**:469–476.
5. Liu Y, Wilcox J: **Effects of surface heterogeneity on the adsorption of CO_2 in microporous carbons.** *Environ Sci Technol* 2012, **46**:1940–1947.
6. Chalbaud C, Robin M, Lombard JM, Martin F, Egermann P, Bertin H: **Interfacial tension measurements and wettability evaluation for geological CO_2 storage.** *Adv Water Resour* 2009, **32**:98–109.
7. Haszeldine RS: **Carbon capture and storage: how green can black be?** *Science* 2009, **325**:1647–1652.
8. Quinonero D, Frontera A, Deya PM: **Feasibility of single-walled carbon nanotubes as materials for CO_2 adsorption: a DFT study.** *J Phys Chem C* 2012, **116**:21083–21092.
9. Zhou H, Park J, Li J-R, Chen Y-P, Yu J, Yakovenko AA, Wang ZU, Sun LB, Balbuena PB, Zhou HC: **A versatile metal-organic framework for carbon dioxide capture and cooperative catalysis.** *Chem Commun* 2012, **48**:9995–9997.
10. Poloni R, Smit B, Neaton JB: **CO_2 capture by metal-organic frameworks with van der Waals density functionals.** *J Phys Chem A* 2012, **116**:4957–4964.
11. Sumida K, Rogow DL, Mason JA, McDonald TM, Bloch ED, Herm ZR, Bae TH, Long JR: **Carbon dioxide capture in metal-organic frameworks.** *Chem Rev* 2012, **112**:724–781.
12. Yi H, Deng H, Tang X, Yu Q, Zhou X, Liu H: **Adsorption equilibrium and kinetics for SO_2, NO, CO_2 on zeolites FAU and LTA.** *J Hazard Mater* 2012, **203–204**:111–117.
13. Yang H, Khan AM, Yuan Y, Tsang SC: **Mesoporous silicon nitride for reversible CO_2 capture.** *Chem Asian J* 2012, **7**:498–502.
14. Qi G, Fu L, Choi BH, Giannelis EP: **Efficient CO_2 sorbents based on silica foam with ultra-large mesopores.** *Energy Environ Sci* 2012, **5**:7368–7375.
15. Zheng B, Yang Z, Bai J, Li Y, Li S: **High and selective CO_2 capture by two mesoporous acylamide-functionalized RHT-type metal-organic frameworks.** *Chem Commun* 2012, **48**:7025–7027.
16. Yu J, Ma Y, Balbuena PB: **Evaluation of the impact of H_2O, O_2, and SO_2 on postcombustion CO_2 capture in metal-organic frameworks.** *Langmuir* 2012, **28**:8064–8071.
17. Wahby A, Ramos-Fernández JM, Martínez-Escandell M, Sepúlveda-Escribano A, Silvestre-Albero J, Rodríguez-Reinoso F: **High-surface-area carbon molecular sieves for selective CO_2 adsorption.** *ChemSusChem* 2010, **3**:974–981.
18. Jiménez V, Ramírez-Lucas A, Díaz JA, Sánchez P, Romero A: **CO_2 capture in different carbon materials.** *Environ Sci Technol* 2012, **6**:7407–7414.
19. Sevilla M, Valle-Vigón P, Fuertes AB: **N-doped polypyrrole-based porous carbons for CO_2 capture.** *Adv Funct Mater* 2011, **21**:2781–2787.
20. Drage TC, Blackman JM, Pevida C, Snape CE: **Evaluation of activated carbon adsorbents for CO_2 capture in gasification.** *Energy Fuel* 2009, **23**:2790–2796.
21. Hao G-P, Li W-C, Qian D, Wang G-H, Zhang W-P, Zhang T, Wang A-Q, Schüth F, Bongard H-J, Lu A-H: **Structurally designed synthesis of mechanically stable poly(benzoxazine-co-resol)-based porous carbon monoliths and their application as high-performance CO_2 capture sorbents.** *J Am Chem Soc* 2011, **133**:11378–11388.
22. Zhang ZQ, Wang K, Atkinson JD, Yan XL, Li X, Rood MJ, Yan Z: **Sustainable and hierarchical porous Enteromorpha prolifera based carbon for CO_2 capture.** *J Hazard Mater* 2012, **229**:183–191.
23. Gutierrez MC, Carriazo D, Ania CO, Parra JB, Ferrer ML, Del Monte F: **Deep eutectic solvents as both precursors and structure directing agents in the synthesis of nitrogen doped hierarchical carbons highly suitable for CO_2 capture.** *Energy Environ Sci* 2011, **4**:3535–3544.
24. Chandra V, Yu SU, Kim SH, Yoon YS, Kim DY, Kwon AH, Meyyappan M, Kim KS: **Highly selective CO_2 capture on N-doped carbon produced by chemical activation of polypyrrole functionalized graphene sheets.** *Chem Commun* 2012, **48**:735–737.
25. Zhou J, Li W, Zhang Z, Xing W, Zhuo S: **Carbon dioxide adsorption performance of N-doped zeolite Y templated carbons.** *RSC Advanc* 2012, **2**:161–167.
26. Nandi M, Okada K, Dutta A, Bhaumik A, Maruyama J, Derks D, Uyama H: **Unprecedented CO_2 uptake over highly porous N-doped activated carbon monoliths prepared by physical activation.** *Chem Commun* 2012, **48**:10283–10285.
27. Wu Z, Webley PA, Zhao D: **Post-enrichment of nitrogen in soft-templated ordered mesoporous carbon materials for highly efficient phenol removal and CO_2 capture.** *J Mater Chem* 2012, **22**:11379–11389.
28. Xing W, Liu C, Zhou ZY, Zhang L, Zhou J, Zhuo SP, Yna Z, Gao H, Wang G, Qiao SZ: **Superior CO_2 uptake of N-doped activated carbon through hydrogen-bonding interaction.** *Energy Environ Sci* 2012, **5**:7323–7327.
29. Maher TP, Schafer HNS: **Determination of acidic functional groups in low-rank coals: comparison of ion-exchange and non-aqueous titration methods.** *Fuel* 1976, **55**:138–140.
30. Presser V, McDonough J, Yeon S-H, Gogotsi Y: **Effect of pore size on carbon dioxide sorption by carbide derived carbon.** *Energy Environ Sci* 2011, **4**:3059–66.
31. Dash R, Chmiola J, Yushin G, Gogotsi Y, Laudisio G, Singer J, Fischer J, Kucheyev S: **Titanium carbide derived nanoporous carbon for energy-related applications.** *Carbon* 2006, **44**:2489–97.
32. Pradhan BK, Sandle NK: **Effect of different oxidizing agent treatments on the surface properties of activated carbons.** *Carbon* 1999, **37**:1323–1332.
33. Zhang Z, Xu M, Wang H, Li Z: **Enhancement of CO_2 adsorption on high surface area activated carbon modified by N_2, H_2 and ammonia.** *Chem Eng J* 2010, **60**:571–577.
34. Chen JP, Wu S: **Acid/base-treated activated carbons: characterization of functional groups and metal adsorptive properties.** *Langmuir* 2004, **20**:2233–2242.
35. Wang J, Heerwig A, Lohe MR, Oschatz M, Borchardt L, Kaskel S: **Fungi-based porous carbons for CO_2 adsorption and separation.** *J Mater Chem* 2012, **22**:13911–13913.
36. Martín CF, Plaza MG, Pis JJ, Rubiera F, Pevida C, Centeno TA: **On the limits of CO_2 capture capacity of carbons.** *Sep Purif Technol* 2010, **74**:225–229.
37. Ribeiro AM, Santos JC, Rodrigues AE, Rifflart S: **Pressure swing adsorption process in coal to Fischer–Tropsch fuels with CO_2 capture.** *Energy Fuel* 2012, **26**:1246–1253.
38. Martín CF, Plaza MG, García S, Pis JJ, Rubiera F, Pevida C: **Microporous phenol–formaldehyde resin-based adsorbents for pre-combustion CO_2 capture.** *Fuel* 2011, **90**:2064–2072.
39. Niwa H, Kobayashi M, Horiba K, Harada Y, Oshima M, Terakura K: **X-ray photoemission spectroscopy analysis of N-containing carbon-based cathode catalysts for polymer electrolyte fuel cells.** *J Power Sources* 2011, **196**:1006–1011.
40. Frisch GWT MJ, Schlegel HB, Scuseria GE, Robb MA, Cheeseman JR, Montgomery JA Jr, Vreven T, Kudin KN, Burant JC, Millam JM, Iyengar SS, Tomasi J, Barone V, Mennucci B, Cossi M, Scalmani G, Rega N, Petersson GA, Nakatsuji H, Hada M, Ehara M, Toyota K, Fukuda R, Hasegawa J, Ishida M, Nakajima Y, Honda Y, Kitao O, Nakai H, Klene M, *et al*: *Gaussian.* Wallingford: Gaussian, Inc; 2004.
41. Kim KH, Kim Y: **Theoretical studies for lewis acid–base interactions and C – H…O weak hydrogen bonding in various CO_2 complexes.** *J Phys Chem A* 2008, **112**:1596–603.

42. Matsuura H, Yoshida H, Hieda M, Yamanaka S-y, Harada T, Shin-ya K, Ohno K: Experimental evidence for intramolecular blue-shifting C – H ⋯ O hydrogen bonding by matrix-isolation infrared spectroscopy. *J Am Chem Soc* 2003, **125**:13910–13911.
43. Yoon S-J, Chung JW, Gierschner J, Kim KS, Choi M-G, Kim D, Park SY: Multistimuli two-color luminescence switching via different slip-stacking of highly fluorescent molecular sheets. *J Am Chem Soc* 2010, **132**:13675–13683.
44. Jeng MLH, DeLaat AM, Ault BS: Infrared matrix isolation study of hydrogen bonds involving carbon-hydrogen bonds: alkynes with nitrogen bases. *J Phys Chem* 1989, **93**:3997–4000.
45. Rozenberg M, Loewenschuss A, Marcus Y: An empirical correlation between stretching vibration redshift and hydrogen bond length. *Phys Chem Chem Phys* 2000, **2**:2699–2702.